

# MD-Dose: A diffusion model based on the Mamba for radiation dose prediction

Linjie Fu<sup>1,2</sup>, Xia Li<sup>4</sup>, and Xiuding Cai<sup>1,2</sup> Yingkai Wang<sup>1,2</sup> Xueyao Wang<sup>1,2</sup>  
Yali Shen<sup>3</sup> Yu Yao<sup>1,2</sup>

- <sup>1</sup> Chengdu Computer Application Institute Chinese Academy of Sciences, China  
<sup>2</sup> University of the Chinese Academy of Sciences, China  
<sup>3</sup> Sichuan University West China Hospital Department of Abdominal Oncology, China  
<sup>4</sup> Radiophysical Technology Center, Cancer Center, West China Hospital, Sichuan University, China

**Abstract.** Radiation therapy is crucial in cancer treatment. Experienced experts typically iteratively generate high-quality dose distribution maps, forming the basis for excellent radiation therapy plans. Therefore, automated prediction of dose distribution maps is significant in expediting the treatment process and providing a better starting point for developing radiation therapy plans. With the remarkable results of diffusion models in predicting high-frequency regions of dose distribution maps, dose prediction methods based on diffusion models have been extensively studied. However, existing methods mainly utilize CNNs or Transformers as denoising networks. CNNs lack the capture of global receptive fields, resulting in suboptimal prediction performance. Transformers excel in global modeling but face quadratic complexity with image size, resulting in significant computational overhead. To tackle these challenges, we introduce a novel diffusion model, MD-Dose, based on the Mamba architecture for predicting radiation therapy dose distribution in thoracic cancer patients. In the forward process, MD-Dose adds Gaussian noise to dose distribution maps to obtain pure noise images. In the backward process, MD-Dose utilizes a noise predictor based on the Mamba to predict the noise, ultimately outputting the dose distribution maps. Furthermore, We develop a Mamba encoder to extract structural information and integrate it into the noise predictor for localizing dose regions in the planning target volume (PTV) and organs at risk (OARs). Through extensive experiments on a dataset of 300 thoracic tumor patients, we showcase the superiority of MD-Dose in various metrics and time consumption. The code is publicly available at [https://github.com/flj19951219/mamba\\_dose](https://github.com/flj19951219/mamba_dose).

**Keywords:** Dose Prediction · Mamba · Diffusion Model · thoracic cancer

## 1 Introduction

Radiation therapy, a critical cancer treatment, necessitates precise and tailored plans to control tumors while sparing healthy tissues [12]. Modern techniques like

Intensity-Modulated Radiation Therapy (IMRT) and Volumetric Modulated Arc Therapy (VMAT) have notably enhanced treatment outcomes [8]. They allow for precise dose sculpting by adjusting beam intensity and angles, conforming to complex tumor shapes while minimizing exposure to healthy tissues. Nonetheless, radiation therapy planning faces challenges: (1) anatomical changes during treatment require plan adaptation, adding complexity. (2) Collaboration between medical physicists and oncologists for plan development is time-consuming, potentially causing delays [1]. (3) Moreover, due to individual differences and complex clinical situations, even experienced expert teams may need help to reach the optimal treatment plan quickly every time [17]. Therefore, automated dose prediction has become particularly important. It can accelerate the treatment process, alleviate the burden on physicians, and provide a better starting point for developing treatment plans, thereby promoting more precise and effective radiation therapy.

Recent researches use deep learning to automate dose distribution map prediction. They employ complex network architectures to learn image features for this task [21, 9, 10, 23, 13]. However, these methods lack high-frequency detail prediction due to loss function averaging [24]. The diffusion model is trainable without prior data distribution knowledge and demonstrates significant potential in dose prediction [2, 3, 4]. As sampling algorithms progress, denoising network research becomes vital for diffusion models. For example, Fu *et al.* [4] uses a transformer-based UNet for dose prediction, outperforming CNN-based models like DiffDP [2]. However, there is a heavier computational burden concerning image size due to the quadratic complexity of the self-attention mechanism in Transformers. Therefore, designing an efficient denoising network is particularly important.

Recent developments in State Space Sequence Models (SSMs) [5], exceptionally structured SSMs (S4) [6], offer a promising solution with efficient performance in processing long sequences. The Mamba model [5] enhances S4 through selective mechanisms and hardware optimization, performing better in dense data domains. Based on the excellent performance of Mamba in long sequence tasks, some researchers have applied Mamba to medical vision tasks, demonstrating its vast potential in modeling complex image distributions [16, 19, 22, 14, 25, 7]. However, research on Mamba in dose prediction is still in its early stages.

In this study, we investigate the feasibility of utilizing Mamba as a denoising network for dose prediction and propose a diffusion model called MD-Dose based on Mamba. MD-Dose consists of a forward process and a reverse process. The forward process gradually introduces noise to the original data until it becomes pure noise, while the reverse process reconstructs the dose distribution map from pure noise. To facilitate this, we develop a Mamba-structured noise predictor named Mamba-UNet to forecast the noise added at each step of the forward process, thereby generating the predicted dose map. Anatomical information provides organ structures and their relative positions. By integrating this anatomical information with noise, we assist the noise predictor in understand-

ing dose constraints between the Planning Target Volume (PTV) and Organs at Risk (OARs), yielding more accurate dose distribution maps.

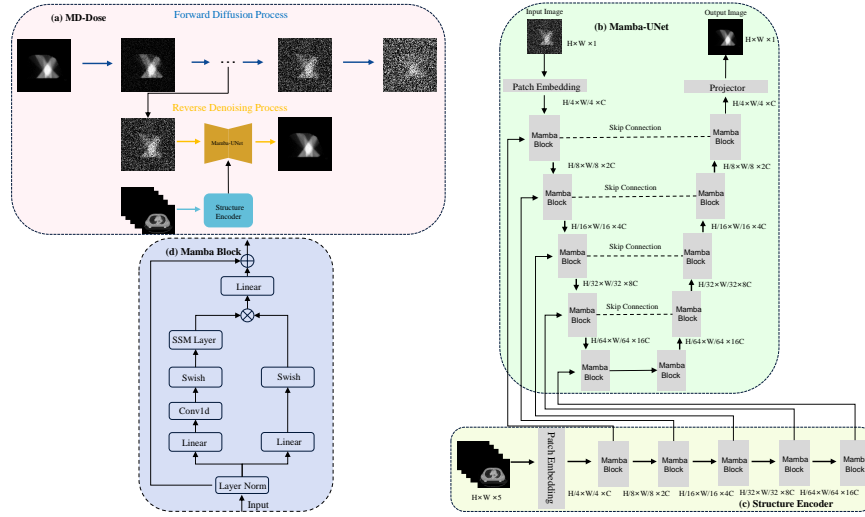


**Fig. 1.** The overview of the proposed MD-Dose, including (a) the overall structure of MD-Dose, encompassing both the forward and backward processes of the diffusion model; (b) the proposed Mamba-UNet; (c) the proposed Structure Encoder; (d) the holistic architecture of the Mamba Block.

The contributions of this paper can be summarized as follows: (1) Based on the exemplary performance in the vision tasks of Mamba, we propose MD-Dose, a novel dose prediction model using Mamba as the denoising network in the diffusion model. To our knowledge, we are the first to introduce Mamba for this task. (2) We develop a Mamba-based structural encoder to extract anatomical information from CT images and organ segmentation masks, guiding the noise predictor to generate more precise predictions. (3) MD-Dose evaluation on a clinical dataset comprising 300 patients with thoracic tumors, showing that our method achieves the best results while consuming fewer time.

## 2 Methodology

Fig. 1 presents the overall network framework of MD-Dose. (a) represents the forward noise addition and backward denoising processes of MD-Dose, (b) illustrates the network architecture of Mamba-UNet, (c) represents the structural encoder architecture, and (d) depicts the network structure of the Mamba Block. We define the dose distribution map as  $x \in \mathbb{R}^{1 \times H \times W}$ , structure image as  $c \in \mathbb{R}^{(2+O) \times H \times W}$ , which 2 represents the image and the PTV, O represents the number of OARs, and H and W define the length and width. During the

forward diffusion process, we add the Gaussian noise to the  $x$  for  $t$  times. In the reverse denoising process, we input  $c$  to the mamba structural encoder to extract the structure feature, and fuse the structure feature with the  $x_t$ , finally input them into the Mamba-UNet to predict the noise in every  $t$ , ultimately generating accurate dose distribution maps.

## 2.1 Score-based Diffusion Generative Models

The framework of MD-Dose is designed based on Score-based diffusion generative models (SDGMs) [20], which learn the distribution of data by simulating the random diffusion process of the data. MD-Dose consists of two main processes: the forward process (diffusion process) and the reverse process (denoising process).

**Forward Process.** The forward process is a stochastic process that gradually transforms data points into random noise. The following stochastic differential equation (SDE) describes this process:

$$d\mathbf{x}_t = \mathbf{f}(\mathbf{x}_t, t)dt + g(t)d\mathbf{w}_t. \quad (1)$$

Here,  $\mathbf{x}_t$  represents the dose distribution map  $x$  at time  $t$ ,  $\mathbf{f}(\mathbf{x}_t, t)$  is a drift term,  $g(t)$  is the diffusion coefficient, and  $\mathbf{w}_t$  is the Brownian motion.

**Reverse Process.** The reverse process is the inverse of the forward process, aiming to reconstruct the dose distribution map  $x$  from noise  $x_t$ . It can be approximated by learning a parameterized model  $\theta$  that attempts to reverse the diffusion process. Express the reverse process as follows:

$$d\mathbf{x}_t = [\mathbf{f}(\mathbf{x}_t, t, \mathbf{c}) - g^2(t, \mathbf{c})\nabla_{\mathbf{x}_t} \log p_t(\mathbf{x}_t|\mathbf{c})]dt + g(t, \mathbf{c})d\bar{\mathbf{w}}_t. \quad (2)$$

Here,  $p_t(\mathbf{x}_t|\mathbf{c})$  represents the probability density function of  $(\mathbf{x}_t)$  at a given condition  $c$ , and  $\bar{\mathbf{w}}_t$  corresponds to the opposite Brownian motion of  $\mathbf{w}_t$ , indicating the stochastic nature of the denoising process.

**Objective Function.** During the training process, we optimize the parameters  $\theta$  by minimizing the reconstruction error and the negative log-likelihood of noise in the reverse process:

$$\mathcal{L}(\theta) = \mathbb{E}_{\mathbf{x}_0, \mathbf{w}_t, \mathbf{c}} [-\log p_\theta(\mathbf{x}_0|\mathbf{x}_t, \mathbf{c}) + \lambda(t, \mathbf{c})\|\mathbf{x}_t - \hat{\mathbf{x}}_t(\mathbf{x}_0, \mathbf{w}_t, \mathbf{c}; \theta)\|^2]. \quad (3)$$

The reconstructed data from noise  $\mathbf{x}_t$  is represented by  $\hat{\mathbf{x}}_t(\mathbf{x}_0, \mathbf{w}_t, \mathbf{c}; \theta)$ .  $\lambda(t)$  is to balance the significance of different time steps.

## 2.2 Mamba-based Denoising Network

Inspired by the recently popular Mamba, we propose the Mamba-UNet. Mamba-UNet utilizes Mamba as a feature extraction block, adopting the encoder and decoder concept from UNet to construct a noise predictor. As shown in Fig. 1(b), Mamba-UNet consists of three parts: 1) a Mamba encoder with multiple Mamba blocks of extracting features at different scales, 2) a Mamba decoder based on

Mamba blocks for predicting the dose distribution map, and 3) skip connections link multiscale features to the decoder for feature reuse. First, we introduce the SSM layer of Mamba.

**SSM Layer.** SSMs map the hidden state  $w(t) \in \mathbb{R}^N$  to a 1-D function or sequence  $y(t) \in \mathbb{R} \rightarrow x(t) \in \mathbb{R}$ , which can be represented by the following linear ordinary differential equation (ODE):

$$\begin{aligned} y'(t) &= Py(t) + Qw(t), \\ x(t) &= Ry(t), \end{aligned} \quad (4)$$

where  $P \in \mathbb{R}^{N \times N}$  is the state matrix, and  $Q$  and  $R \in \mathbb{R}^N$  are parameters, with  $y'(t) \in \mathbb{R}^N$  representing the implicit latent state.

S4 and Mamba are discrete versions of continuous systems, making them more suitable for deep learning scenarios. Specifically, S4 introduces a time scale parameter  $\Delta$  and uses a fixed discretization rule to transform  $A$  and  $B$  into discrete parameters  $\bar{P}$  and  $\bar{Q}$ . They are defined as follows:

$$\begin{aligned} \bar{P} &= \exp(\Delta P), \\ \bar{Q} &= (\Delta P)^{-1}(\exp(\Delta P) - I) \cdot \Delta Q. \end{aligned} \quad (5)$$

After discretizing  $P$  and  $Q$ , linear recursion is used for rewriting:

$$\begin{aligned} y_t &= \bar{P}y(t) + \bar{Q}w(t), \\ x_t &= Ry(t). \end{aligned} \quad (6)$$

Finally, the output through global convolution to calculate:

$$\begin{aligned} \bar{H} &= (R\bar{Q}, C\bar{P}\bar{Q}, \dots, R\bar{P}N^{-1}\bar{Q}), \\ x &= y * \bar{H}, \end{aligned} \quad (7)$$

where  $N$  is the length of the input sequence  $y$ , and  $\bar{H} \in \mathbb{R}^M$  is a structured convolution kernel.

**Mamba Block.** Fig. 1(d) illustrates the comprehensive overview of the Mamba Block. Similar to the Transformer, we make the noisy image through a Patch Embedding, flattening and transposing the features with a shape of  $(B, C, H, W)$  to  $(B, L, C)$ , where  $L = H \times W$ , and then input it into the Mamba Block. The Mamba Block initially inputs the noisy image to a layer normalization and sends it to two parallel branches.

In the first branch, the feature is linearly expanded to  $(B, 2L, C)$  followed by successive 1D convolution layers, the Swish activation function, and the SSM layer. The second branch also expands the features to  $(B, 2L, C)$ , followed by a linear layer and Swish activation function. Next, we combine the features from both branches using Hadamard multiplication. Subsequently, the features are projected back to the original shape  $(B, L, C)$ , reshaped, and transposed to  $(B, C, H, W)$ . Finally, we encode the current time  $t$  and add it to the output features. Additionally, the channel count doubles after each down-sampling, while after each up-sampling, the channel count halves.

**Structure Encoder.** During encoding, we introduce an additional structural encoder to extract features from structural images and incorporate structural information into the noisy images to guide Mamba-UNet in restoring dose distribution maps. The structural encoder mirrors the encoder architecture of Mamba-UNet, comprising four down-sampling Mamba Blocks. As depicted in Fig. 1(c), we feed the structural images into the structural encoder. Subsequently, we add the output of each Mamba block in the structural encoder to the corresponding Mamba block output in Mamba UNet to fuse information.

### 2.3 Training Details

We implement MD-Dose using PyTorch on an NVIDIA GeForce RTX 3090. Throughout the experiment, we set the batch size to 16 and use Adam[11] as the optimizer. The model undergoes training for 1500 epochs, with the learning rate initially set at 1e-2. It starts to decay linearly at the beginning of every epoch after 750 epochs, down to 1e-4, to accelerate convergence and prevent getting stuck in local minima. We set the parameters  $\lambda_1$  and  $\lambda_2$  to 1.0 and the diffusion step parameter T to 1000.

## 3 Experiments & Results

**Datasets and Evaluation Metrics.** We conduct experiments on an in-house dataset to assess the performance of MD-Dose. The dataset comprises CT images, PTV and OARs segmentation masks, and dose distribution maps from 300 patients with thoracic tumors. OARs included the heart, lungs, and spinal cord. The dataset is randomly split into training (200 patients), validation (20 patients), and test (80 patients) sets. We slice the 3D CT image into 2D slices, resize them to  $256 \times 256$ , and utilize images with dose as inputs to the network. The dataset used in this study is from \*\*, and the ethics number is \*\*.

We evaluate the performance of the MD-Dose using the Dose Score [15], the DVH Score [15] and the Homogeneity Index (HI) [2].

**Comparison with State-Of-The-Art Methods.** We compare MD-Dose with C3D [15], HD-UNet [18], DiffDP [2], and SP-DiffDose [4] to validate its effectiveness. The experimental results from Table 1 demonstrate that MD-Dose outperforms the existing SOTA in all metrics. Specifically, MD-Dose has a Dose Score of 1.980, a DVH Score of 1.572, and an HI index of 0.285. In addition, we use paired t-tests to assess the statistical significance of the improvements brought by MD-Dose compared to other methods. The experimental results in Table 3 indicate that the enhancement in MD-Dose results is statistically significant ( $p < 0.05$ ).

To further investigate the performance of MD-Dose, we present visual results in Fig. 2, showing dose distribution maps predicted by all methods, ground truth (GT), and dose error maps between all methods and GT. MD-Dose achieves the best visual quality with more apparent high-frequency details. Moreover, the

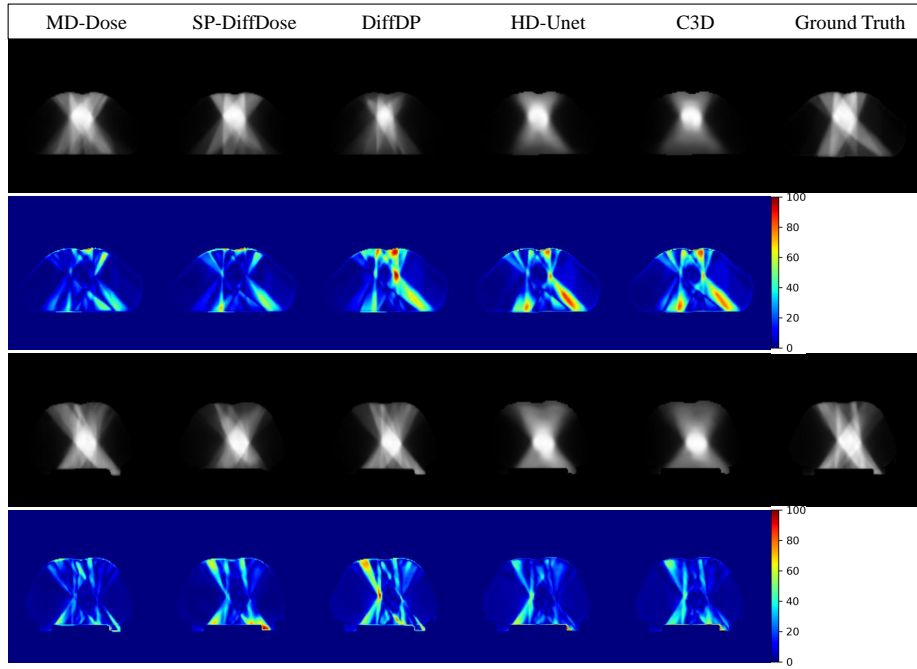


**Fig. 2.** Visual comparisons with state-of-the-art (SOTA) methods include two sets. The first and third rows illustrate predicted dose distribution maps, and the second and fourth rows display maps depicting dose errors. The last column represents the ground truth.

**Table 1.** Quantitative comparison results with diffusion model methods in terms of Parameters and Inference Time. The best results are highlighted in bold. \* indicates that our method significantly outperforms the compared method with a p-value of less than 0.05, as determined by a paired t-test.

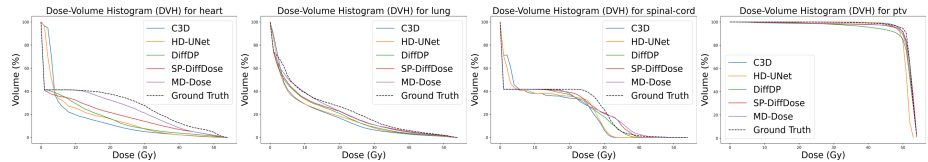
Methods	Dose Score↓	DVH Score↓	HI↓
C3D [15]	4.630±2.161*	3.618±0.778*	0.594±0.150*
HD-UNet [18]	4.172±1.749*	3.195±0.608*	0.560±0.122*
DiffDP [2]	2.120±1.225*	1.858±0.292*	0.334±0.101*
SP-DiffDose [4]	2.000±1.131*	1.775±0.278*	0.292±0.068*
MD-Dose	<b>1.980±1.149</b>	<b>1.572±0.239</b>	<b>0.285±0.054</b>

dose error maps of MD-Dose are the lightest, indicating minimal differences compared to GT.

Furthermore, we compute DVH curves for OARs and the PTV, where closer proximity to GT indicates better prediction results. Fig. 3 illustrates that MD-Dose’s DVH curves are the most comparable to GT among all OARs and the PTV.

**Table 2.** Quantitative comparison results with diffusion model methods in terms of Parameters and Inference Time. The best results are highlighted in bold.

	DiffDP	SP-DiffDose	MD-Dose
Parameter	37.36 M	84.11 M	<b>30.47 M</b>
Inference Time	0.25 sec/iter	0.30 sec/iter	<b>0.18 sec/iter</b>

**Fig. 3.** Visualize the DVH curves of all methods, encompassing curves for the PTV, Heart, Lung, and Spinal Cord.**Table 3.** Quantitative results of ablative studies. Conv-SE, Trans-SE, and Mamba-SE respectively represent structure encoders using Convolution, Transformer, and Mamba architectures. Mark the best results in bold.

Conv-SE	Trans-SE	Mamba-SE	Dose Score↓	DVH Score↓	HI↓
			2.076	1.787	0.298
✓			1.998	1.658	0.294
	✓		1.995	1.627	0.289
		✓	<b>1.980</b>	<b>1.572</b>	<b>0.285</b>

Finally, we show the computational advantages and speed brought by Mamba. Table 2 presents the number of parameters and inference time for the three methods based on the diffusion model. Compared to DiffDP and SP-DiffDose, MD-Dose demonstrates shorter inference times with fewer parameters, indicating that MD-Dose is an efficient dose prediction method.

**Ablation Study.** We conduct ablation experiments to demonstrate the effectiveness of the structure encoder and the superiority of the Mamba architecture. As shown in Table 3, the structure encoder improves the performance across all metrics, validating its effectiveness. Furthermore, employing the structure encoder with the Mamba architecture yields the best predictive performance, demonstrating the superiority of the Mamba architecture.

## 4 Conclusion

In this paper, we propose a novel radiation dose prediction method called MD-Dose. MD-Dose utilizes Mamba as a denoising network to predict dose distribution maps for cancer patients. It also incorporates a Mamba encoder to extract structural information from anatomical images and integrate it into the denoising network, resulting in higher-quality dose distribution maps. MD-Dose can provide dose distribution maps with more high-frequency details compared to



other methods, surpassing other diffusion model methods regarding inference speed. Through our approach, we can utilize the generated dose distribution maps as the initial solution for clinical radiotherapy planning, easing the burden on physicists and physicians and assisting cancer patients in undergoing more effective and precise treatment planning.

**Acknowledgements.** This work was supported by \*\*\* (\*\*\*) and \*\*\* (\*\*\*) .

## Bibliography

- [1] Braam, P.M., Terhaard, C.H., Roesink, J.M., Raaijmakers, C.P.: Intensity-modulated radiotherapy significantly reduces xerostomia compared with conventional radiotherapy. *International Journal of Radiation Oncology\* Biology\* Physics* **66**(4), 975–980 (2006)
- [2] Feng, Z., Wen, L., Wang, P., Yan, B., Wu, X., Zhou, J., Wang, Y.: Diffdp: Radiotherapy dose prediction via a diffusion model. In: *International Conference on Medical Image Computing and Computer-Assisted Intervention*. pp. 191–201. Springer (2023)
- [3] Feng, Z., Wen, L., Xiao, J., Xu, Y., Wu, X., Zhou, J., Peng, X., Wang, Y.: Diffusion-based radiotherapy dose prediction guided by inter-slice aware structure encoding. *arXiv preprint arXiv:2311.02991* (2023)
- [4] Fu, L., Li, X., Cai, X., Wang, Y., Wang, X., Yao, Y., Shen, Y.: Sp-diffdose: A conditional diffusion model for radiation dose prediction based on multi-scale fusion of anatomical structures, guided by swintransformer and projector. *arXiv preprint arXiv:2312.06187* (2023)
- [5] Gu, A., Dao, T.: Mamba: Linear-time sequence modeling with selective state spaces. *arXiv preprint arXiv:2312.00752* (2023)
- [6] Gu, A., Goel, K., Ré, C.: Efficiently modeling long sequences with structured state spaces. *arXiv preprint arXiv:2111.00396* (2021)
- [7] Guo, T., Wang, Y., Meng, C.: Mambamorph: a mamba-based backbone with contrastive feature learning for deformable mr-ct registration. *arXiv preprint arXiv:2401.13934* (2024)
- [8] Hussein, M., Heijmen, B.J., Verellen, D., Nisbet, A.: Automation in intensity modulated radiotherapy treatment planning—a review of recent innovations. *The British journal of radiology* **91**(1092), 20180270 (2018)
- [9] Jhanwar, G., Dahiya, N., Ghahremani, P., Zarepisheh, M., Nadeem, S.: Domain knowledge driven 3d dose prediction using moment-based loss function. *Physics in Medicine & Biology* **67**(18), 185017 (2022)
- [10] Jiao, Z., Peng, X., Wang, Y., Xiao, J., Nie, D., Wu, X., Wang, X., Zhou, J., Shen, D.: Transdose: Transformer-based radiotherapy dose prediction from ct images guided by super-pixel-level gcn classification. *Medical Image Analysis* **89**, 102902 (2023)
- [11] Kingma, D.P., Ba, J.: Adam: A method for stochastic optimization. *arXiv preprint arXiv:1412.6980* (2014)
- [12] Lee, C.Y., Chang, C.C., Yang, H.Y., Chiang, P.Y., Tsang, Y.W.: Intensity modulated radiotherapy delivers competitive local control rate with limited acute toxicity in the adjuvant treatment of rectal cancer. *Japanese Journal of Clinical Oncology* **48**(7), 653–660 (2018)
- [13] Li, F., Niu, S., Han, Y., Zhang, Y., Dong, Z., Zhu, J.: Multi-stage framework with difficulty-aware learning for progressive dose prediction. *Biomedical Signal Processing and Control* **82**, 104541 (2023)

- [14] Liu, J., Yang, H., Zhou, H.Y., Xi, Y., Yu, L., Yu, Y., Liang, Y., Shi, G., Zhang, S., Zheng, H., et al.: Swin-umamba: Mamba-based unet with imagenet-based pretraining. arXiv preprint arXiv:2402.03302 (2024)
- [15] Liu, S., Zhang, J., Li, T., Yan, H., Liu, J.: A cascade 3d u-net for dose prediction in radiotherapy. *Medical physics* **48**(9), 5574–5582 (2021)
- [16] Ma, J., Li, F., Wang, B.: U-mamba: Enhancing long-range dependency for biomedical image segmentation. arXiv preprint arXiv:2401.04722 (2024)
- [17] Nelms, B.E., Robinson, G., Markham, J., Velasco, K., Boyd, S., Narayan, S., Wheeler, J., Sobczak, M.L.: Variation in external beam treatment plan quality: an inter-institutional study of planners and planning systems. *Practical radiation oncology* **2**(4), 296–305 (2012)
- [18] Nguyen, D., Jia, X., Sher, D., Lin, M.H., Iqbal, Z., Liu, H., Jiang, S.: 3d radiotherapy dose prediction on head and neck cancer patients with a hierarchically densely connected u-net deep learning architecture. *Physics in medicine & Biology* **64**(6), 065020 (2019)
- [19] Ruan, J., Xiang, S.: Vm-unet: Vision mamba unet for medical image segmentation. arXiv preprint arXiv:2402.02491 (2024)
- [20] Song, Y., Sohl-Dickstein, J., Kingma, D.P., Kumar, A., Ermon, S., Poole, B.: Score-based generative modeling through stochastic differential equations. arXiv preprint arXiv:2011.13456 (2020)
- [21] Wang, J., Hu, J., Song, Y., Wang, Q., Zhang, X., Bai, S., Yi, Z.: Vmat dose prediction in radiotherapy by using progressive refinement unet. *Neurocomputing* **488**, 528–539 (2022)
- [22] Wang, Z., Zheng, J.Q., Zhang, Y., Cui, G., Li, L.: Mamba-unet: Unet-like pure visual mamba for medical image segmentation. arXiv preprint arXiv:2402.05079 (2024)
- [23] Wen, L., Xiao, J., Tan, S., Wu, X., Zhou, J., Peng, X., Wang, Y.: A transformer-embedded multi-task model for dose distribution prediction. *International Journal of Neural Systems* pp. 2350043–2350043 (2023)
- [24] Xie, Y., Yuan, M., Dong, B., Li, Q.: Diffusion model for generative image denoising. arXiv preprint arXiv:2302.02398 (2023)
- [25] Xing, Z., Ye, T., Yang, Y., Liu, G., Zhu, L.: Segmamba: Long-range sequential modeling mamba for 3d medical image segmentation. arXiv preprint arXiv:2401.13560 (2024)